J. Membrane Biol. 186, 1–12 (2002)
DOI: 10.1007/s00232-001-0130-1

The Journal of
Membrane
Biology

Functional Expression of GFP-linked Human Heart Sodium Channel (hH1) and Subcellular Localization of the α Subunit in HEK293 Cells and Dog Cardiac Myocytes

T. Zimmer,[1] C. Biskup,[1] S. Dugarmaa,[1] F. Vogel,[2] M. Steinbis,[1] T. Böhle,[1,*] Y.S. Wu,[3] R. Dumaine,[3] K. Benndorf[1]

[1]Friedrich Schiller University Jena, Institute of Physiology II, Teichgraben 8, 07740 Jena, Germany.
[2]Max Delbrück Centre for Molecular Medicine, Robert-Rössle-Str. 10, 13125 Berlin, Germany.
[3]Masonic Medical Research Laboratory, Utica NY 13501, USA.

Received: 15 May 2001/Revised: 29 September 2001

Abstract. Recent evidence suggests that biosynthesis of the human heart Na^+ channel (hH1) protein is rapidly modulated by sympathetic interventions. However, data regarding the intracellular processing of hH1 in vivo are lacking. In this study we sought to establish a model that would allow us to study the subcellular localization of hH1 protein. Such a model could eventually help us to better understand the trafficking of hH1 in vivo and its potential role in cardiac conduction. We labeled the C-terminus of hH1 with the green fluorescent protein (GFP) and compared the expression of this construct (hH1-GFP) and hH1 in transfected HEK293 cells. Fusion of GFP to hH1 did not alter its electrophysiological properties. Confocal microscopy revealed that hH1-GFP was highly expressed in intracellular membrane structures. Immuno-electronmicrographs showed that transfection of hH1-GFP and hH1 induced proliferation of three types of endoplasmic reticulum (ER) membranes to accommodate the heterologously expressed proteins. Labeling with specific markers for the ER and the Golgi apparatus indicated that the intracellular channels are almost exclusively retained within the ER. Immunocytochemical labeling of the Na^+ channel in dog cardiomyocytes showed strong fluorescence in the perinuclear region of the cells, a result consistent with our findings in HEK293 cells. We propose that the ER may serve as a reservoir for the cardiac Na^+ channels and that the transport from the ER to the Golgi apparatus is among the rate-limiting steps for sarcolemmal expression of Na^+ channels.

Key words: ER proliferation — Golgi apparatus — Heart ventricle — Immunoelectron microscopy — Voltage-gated Na^+ channel

Introduction

Voltage-gated Na^+ channels are responsible for the rapid increase in membrane Na^+ permeability during the upstroke of action potentials in excitable tissues (Catterall, 1992). These channels are heteromeric complexes consisting of a pore-forming α subunit and associated β subunits. During the last decade, various Na^+-channel α and β subunits have been cloned from different mammalian tissues (Brammar, 1999; Kazen-Gillespie et al., 2000; Morgan et al., 2000) and kinetic parameters of individual Na^+ channels have been extensively studied upon heterologous expression.

In contrast to the broad knowledge of the electrophysiology of Na^+ channels, the regulation of biosynthetic pathways leading to functional channels in the plasma membrane is less well understood. Schmidt and Caterall (1986) demonstrated the presence of an intracellular pool of neuronal Na^+ channels in developing rat brain and suggested the existence of a control mechanism for the trafficking of Na^+ channels to the plasma membrane. The same group (Schmidt & Caterall, 1986, 1987) also showed that the α subunit becomes heavily glycosylated in the Golgi apparatus. In the mammalian heart, similar studies have not been performed, but recent evidence indicates that the trafficking of the human heart Na^+ channel (hH1) is controlled by cAMP-dependent

Present address: T. Böhle, Universität Köln, Klinik für Innere Medizin III, Josef-Stelzmann-Str. 9, 50924 Köln, Germany

Correspondence to: T. Zimmer; email: tzim@mti-n.uni-jena.de

protein kinase (protein kinase A [PKA]; Zhou et al., 2000). These authors demonstrated that PKA stimulation resulted in a 30% increase of heterologously expressed hH1 channels at the plasma membrane after 30 minutes. Such a rapid increase in the number of channels available at the plasma membrane is difficult to reconcile with mechanisms involving up-regulation of both transcription and translation. The aim of this study was to identify post-transcriptional steps in the expression of hH1 and to establish a trafficking model for future studies on subunit assembly of Na^+ channels. For this purpose, we fused variants of the green fluorescent protein (GFP) to the hH1 α subunit and compared the expression of this fusion construct with hH1 alone in transiently transfected hEK293 cells. We found that the electrophysiological properties and the subcellular distribution of hH1 were not altered by the presence of GFP. Using confocal laser-scanning and immunoelectronmicroscopy we observed large concentrations of the hH1-GFP protein within intracellular membranes belonging to the endoplasmic reticulum (ER) and a lower density of channels in the plasma membrane. hH1-GFP and hH1 induced proliferation of ER membranes to accommodate the amount of protein synthesized. The channel density within the Golgi apparatus was significantly lower than in the ER. Native cardiac Na^+ channel proteins in dog ventricular myocytes concentrated around the nuclei of the cell, similarly as the recombinant channels in HEK293 cells. Implications for a possible rate-limiting role of the ER-to-Golgi transport system in the expression of hH1 and a possible role of the ER as a storage organelle are discussed.

Materials and Methods

Plasmid Constructions

To construct plasmid pTSV40-hH1, which allowed the simultaneous expression of hH1 and the GFP marker, the hH1 cDNA (Gellens et al., 1992) was inserted as a *Hind*III/*Xba*I fragment into the *Asp*718/*Spe*I site of plasmid pTracerSV40 (Invitrogen) after Klenow treatment of the *Hind*III and *Asp*718 sites. To obtain vector pEGFPN2-hH1, the coding region of hH1 was ligated as a *Hind*III/*Tth*111I fragment into the *Hind*III/*Bam*HI site of plasmid pEGFP-N2 (Clontech). The *Tth*111I and *Bam*HI sites were treated with Klenow enzyme to allow for respective blunt end ligation. The expected amino acid of the hH1-GFP fusion encoded by pEGFPN2-hH1 is $hH1_{(1–1978)}$-RIHRPVAT-$GFP_{(1–239)}$ (the linker region is underlined). For simultaneous detection of hH1 and the ER marker (encoded by pECFP-ER from Clontech) or the Golgi marker (encoded by pEYFP-Golgi from Clontech) in a transfected cell, the GFP variant was replaced in pEGFPN2-hH1 for the YFP- or CFP-coding regions, respectively. This modification was done by a PCR approach. First, plasmid pEYFP-Golgi (Clontech) and pECFP-ER (Clontech) were used as templates for the amplification of the respective GFP sequences. Then, the full-length coding region of hH1 was fused in a recombinant PCR step directly to the YFP or CFP fragment to create the hH1-YFP and hH1-CFP fusion, respectively. These fragments were digested by *Not*I/*Asp*I and inserted into the corresponding *Not*I/*Asp*I site of pEGFPN2-hH1 to create pEYFP-hH1 and pECFP-hH1. The fusion constructs were expected to encode the following protein sequences: $hH1_{(1–2016)}$-$YEP_{(1–239)}$ (hH1–YFP) and $hH1_{(1–2016)}$-$CFP_{(1–239)}$ (hH1-CFP). The correctness of the DNA constructs was checked by the dideoxy DNA sequencing method (Sanger, Nicklen & Coulsen, 1977). Preparation, digestion and ligation of DNA were carried out according to established procedures (Sambrook, Fritsch & Maniatis, 1989).

The ER marker (termed CFP-ER) is encoded by plasmid pECFP-ER (Clontech) and contains the cyan variant of GFP (CFP), the ER-targeting sequence of calreticulin and the ER-retrieval sequence KDEL. This fusion is a soluble protein that localizes in the lumen of the ER in transfected cells but not in the Golgi apparatus. The Golgi marker (termed YFP-Golgi) is encoded by pEYFP-Golgi (Clontech). It contains the yellow variant of GFP (YFP) and the N-terminal 81 amino acids of the human beta 1,4-galactosyltransferase. This N-terminal part contains the membrane-anchoring signal peptide that targets the fusion protein to the trans-medial region of the Golgi apparatus.

Transfection of HEK293 Cells

Plasmid DNA for transfection was purified by the Plasmid Midi Kit (Qiagen, Hilden, Germany). HEK293 cells were transfected by a standard calcium-phosphate precipitation method using in total 1 to 3 μg of purified plasmid DNA per transfection (60-mm cell culture dishes). After an incubation time of 24 hr the transfection mixture was removed, and the cells were seeded onto poly-L-lysine-coated glass coverslips and cultured in fresh growth medium for 1–2 days. Then, respective cells were used for GFP imaging (Figs. 3*B* and 7), immuno-electronmicroscopy (Figs. 4 and 5), and for the electrophysiological recordings (Figs. 1 and 2). When studying the time-dependency of hH1-GFP expression (cell in Fig. 3*A*), transfection was performed with the liposome reagent DMRIE-C (Gibco BRL). HEK293 cells were incubated with 0.5 μg plasmid DNA per ml transfection mixture for 5 hours and then transferred to fresh MEM medium (Gibco BRL). The expression of hH1-GFP was traced as indicated in the Results section.

Dissociation of Cardiac Myocytes

Cardiac myocyte dissociation from adult male mongrel dog hearts was carried out as previously described (Zygmunt, Goodrow & Weigel, 1998). Euthanasia, care and maintenance followed the guidelines established by the US National Institutes of Health (NIH) and the Institutional Animal Care and Use Committee of the Masonic Medical Research Laboratory.

Following dissociation, the cells were resuspended in a cardioplegic solution containing (in mM): 132 NaCl, 20 HEPES/NaOH, 3.3 $MgSO_4 \times 7H_2O$, 11.1 D-Glucose, 5 KCl, 0.5 $CaCl_2$, 1.5% BSA and stored at 4°C for 1 to 3 hours. In instances where the yield of viable cells was low, the fraction was enriched by purification on a Percoll gradient as previously described (Heathers et al., 1987). A ratio of 70% viable cells was deemed adequate to carry the immunodetection procedure.

Electrophysiology

All recordings were performed with the patch-clamp technique on the stage of an inverted microscope (Axiovert 100, Zeiss, Germany) using an Axopatch 200B amplifier (Axon Instruments, Foster City, CA). When studying hH1 channels, GFP was co-expressed using vector pTSV40-hH1, and we only investigated cells that showed

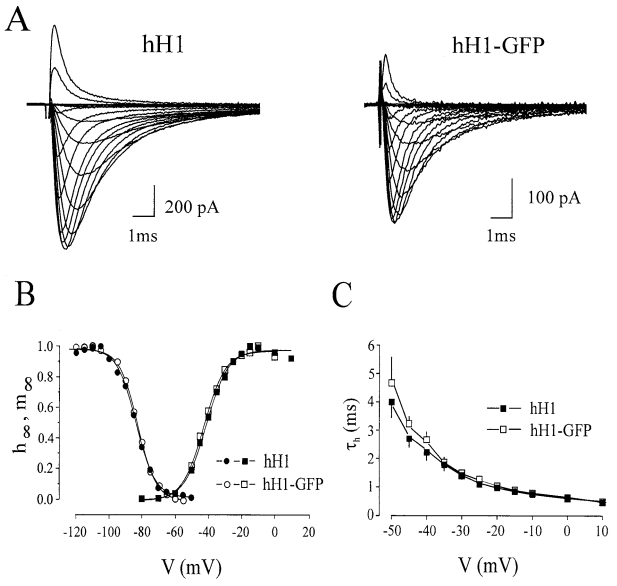

Fig. 1 *(A)*. Representative whole-cell Na^+ currents generated by hH1 and hH1-GFP channels. The currents were elicited by test potentials from −80 to 40 mV in 10-mV increments from a holding potential of −120 mV. The pulsing frequency was 5 Hz. (*B*) Steady-state activation (squares) and inactivation (circles) as a function of voltage in two representative cells. Steady-state activation (m_∞) was evaluated by fitting normalized conductance-voltage values from currents recorded as in *A* to a Boltzmann distribution ($m_\in fty = \{1 + \exp[-(V - V_h)/s]\}^{-1}$). Steady-state inactivation (h_∞) was investigated with a double-pulse protocol consisting of 500-msec conditioning prepulses between −120 and −30 mV followed by a constant test pulse of 10 msec duration to −30 mV (pulsing frequency 0.5 Hz). The amplitude of peak I_{Na} during the test pulse was normalized to the maximum peak current and plotted as function of the prepulse potential. Data were fitted to the Boltzmann equation $h_\infty = \{1 + \exp[(V - V_h)/s]\}^{-1}$. Symbols: *V*, membrane test potential; V_h, mid-activation or inactivation potential; *s*, slope factor in mV. (*C*) Time constant of inactivation as function of voltage. The individual values (± SEM) were obtained either from monoexponential fits or from the fast component of

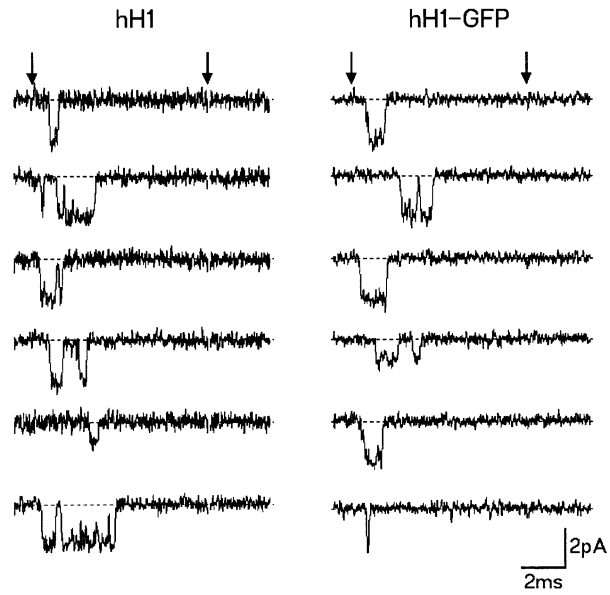

Fig. 2. Single-channel recordings in hH1 and hH1-GFP in cell-attached patches. Channel activity was recorded during 8-msec pulses to a test potential of −40 mV from a holding potential of −120 mV (beginning and ending of the pulses are indicated by the arrows in the upper traces).

fluorescence when excited with UV light. In the case of the hH1-GFP channels, the cells were selected by the fluorescence generated by the construct itself. All measurements were carried out at room temperature. Whole-cell currents were measured with standard techniques (Hamill et al., 1981). The bath solution contained (mM): 20.0 NaCl, 120.0 CsCl, 0.1 $CaCl_2$, 1.0 $MgCl_2$, 10.0 HEPES, 0.001 nitrendipine, pH 7.4 (CsOH). Nitrendipine (1 mM stock solution in ethanol) was added to exclude any overlap with currents through incidentally present endogenous L-type Ca^{2+} channels. Glass pipettes were pulled from borosilicate glass and heat-polished. The pipette resistance was between 1 and 2 MΩ when filled with the pipette solution containing (mM): 10.0 NaCl, 130.0 CsCl, 10.0 EGTA, 10.0 HEPES, pH 7.3 (CsOH). Series resistance compensation was adjusted so that any oscillations were avoided, leaving at most 20% of the series resistance uncompensated. Currents were on-line filtered with a cut-off frequency of 10 kHz (4-pole Bessel).

Single-channel recording was performed with thick-walled pipettes prepared from borosilicate glass tubing with an outer diameter of 2.0 mm and an inner diameter of 0.5 mm. The pipettes were shortened to a total length of 8 mm and then glued to a small pipette holder fabricated completely from silver. The technique has been described in detail by Benndorf (1995) and Böhle et al. (1998). Pipettes were used repetitively by breaking the tips on the floor of the chamber (Böhle & Benndorf, 1994). The pipette resistance was between 10 and 50 MΩ when filled with the following solution (mM): 255.0 NaCl, 2.5 $CaCl_2$, 4.0 KCl, 1.0 $MgCl_2$, 5.0 HEPES, pH 7.3 (NaOH). The Na^+ concentration in the pipette solution was set to a value much higher than the physiological concentration to enlarge the unitary currents. The bath solution contained (mM) 230.0 KCl, 20.0 CsCl, 1.0 $MgCl_2$, 10.0 EGTA, 10.0 HEPES, pH 7.3 (KOH). Recordings were on-line filtered with a cut-off frequency of 20 kHz (4-pole Bessel) and later filtered to the final cut-off frequency of 5–8 kHz with a Gaussian filter routine. Recording and analysis of the data were performed on a PC with the ISO2 software (MFK, Niedernhausen, Germany). The sampling rate was generally 50 kHz.

Statistics

Data are presented as mean ± SEM. Student's *t*-test was used to test for statistical significance. Statistical significance was assumed for $P < 0.05$.

Immuno-Electronmicroscopy

Transfected HEK293 cells were fixed in a mixture of 4% formaldehyde/0.5% glutaraldehyde and processed for frozen sectioning essentially as described by Tokuyasu (1989). Sections were labelled with antibodies against hH1 (1:100 dilution) or GFP (1:200 dilution), followed by decoration with protein A anti-rabbit-gold (Dianova, Hamburg). Labelling of hH1 was done using the polyclonal anti-pan Na^+ channel antibody from Alomone Labs (Jerusalem, Israel). This antibody is directed against the conserved motif TEEQKKYYNAMKKLGSKK located in the linker region between domain III and IV. Anti-GFP antibody was purchased from Clontech. Finally, the freeze-thawed sections were stained and

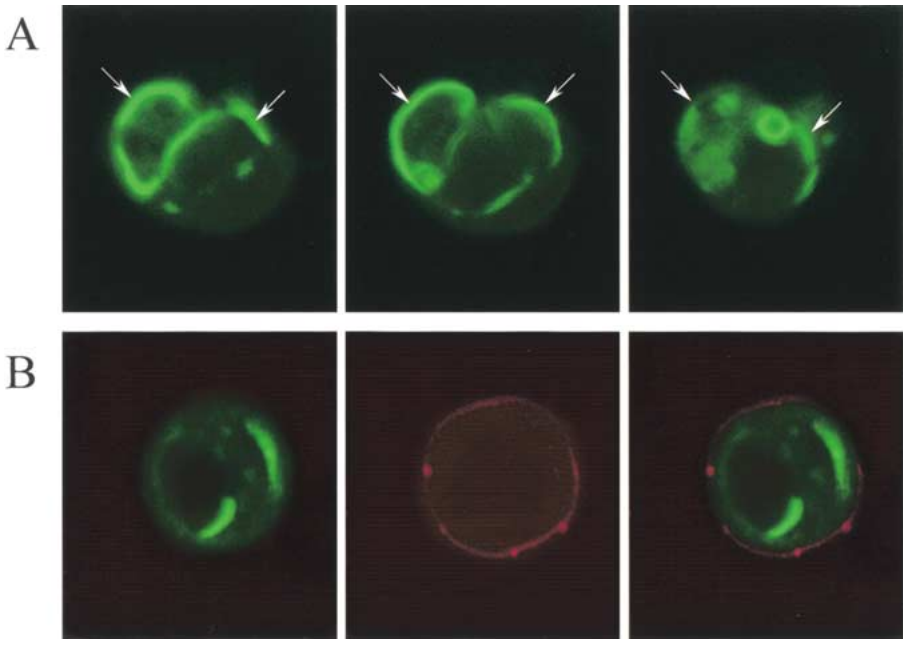

Fig. 3. HEK293 cells expressing hH1-GFP observed by confocal laser-scanning microscopy. (*A*) Fluorescence pattern observed in different planes of one individual cell (2.7 μm distance between each layer), indicating the three-dimensional nature of the membranous semicircle-like structures (arrows). (*B*) Simultaneous staining of the plasma membrane. The left panel shows the fluorescence pattern generated by hH1-GFP. The plasma membrane was stained with FM1-43 as described in the Methods section (panel in the middle). Both images were superimposed (right panel) to demonstrate that only a minor portion of the total green fluorescence colocalized with the cell surface.

stabilized using a freshly prepared mixture of 3% tungstosilicic acid hydrate (STA, Fluka) and 2.5% polyvinylalcohol (Mr 10,000; Sigma; Tokuyasu, 1989). As controls for the immunoreaction with antibodies, the sections were incubated directly with protein A-gold omitting reaction with primary antibodies, or cells not expressing the antigens were used.

Confocal Laser-Scanning Microscopy

Confocal imaging of HEK293 cells was performed with a Zeiss LSM 510 (Carl Zeiss GmbH, Jena, Germany) and dog cardiac myocytes were scanned with an Olympus Fluoview (Olympus, Japan). For plasma-membrane staining, transfected cells were incubated for 10 minutes at room temperature (25°C) in a depolarizing medium (140 mM K^+, 10 mM Na^+) containing the styrylpyridinium dye FM1-43 (Molecular Probes, Eugene, OR) at a concentration of 3 μM. Afterwards, cells were washed several times with PBS and superfused with MEM medium (Gibco BRL).

Experiments were performed with a Zeiss C-Apochromat 63x (NA 1.20) water immersion objective or an Olympus PLAPO60x (NA 1.4) oil immersion objective. For excitation of GFP and Alexa 488 dye, the 488 nm line of a 15 mW Ar-Ion-Laser was used. The FM1-43 and propidium iodine (PI) dyes were excited with the 543 nm line of a 0.5 mW HeNe-Laser. Fluorescence of GFP alone and Alexa 488 was observed with a 505 nm long pass filter and a narrow band filter (510–530 nm), respectively. For simultaneous recording of the GFP and the membrane dye fluorescence, the emitted light was passed through a dichroic mirror (Zeiss FT 545). GFP and Alexa 488 fluorescence was detected at 505–530 nm (green channel). FM1-43 and PI fluorescence as well as the long-wavelength emission lines of GFP were recorded at wavelengths > 560 nm (red channel). The confocal aperture was adjusted to give optical sections between 0.8 and 1.0 μm as stated. FM1-43 fluorescence signals were calculated by correcting the fluorescence signals registered in the red channel for GFP. To remove FM1–43 fluorescence signals coming from FM1–43 molecules bound to the poly-L-lysine-coated cover plates, the images were subjected to an erosion/dilation algorithm. CFP and YFP were excited with the 458 nm and 514 nm line of an Argon laser, respectively. Emission signals were successively recorded through a 470–500 nm narrow band filter (CFP) and a 530 nm long pass filter (YFP). Cotransfected cells and cardiomyocytes were first selected under epifluorescence using appropriate sets of dichroic mirrors and filters (AHF Analysentechnik AG, Tübingen, Germany), and then studied by laser-scanning microscopy.

Transmitted Differential Interference Contrast (DIC-Nomarski) images were simultaneously obtained with the Alexa 488 signal on a separate channel of the Fluoview laser-scanning microscope using the standard set of interference filters, polarizers and condenser attachments of an IX70 inverted microscope (Olympus, Japan).

Immunocytochemical Detection of SCN5A Channels in Cardiomyocytes

Following dissociation and storage at 4°C, the cardioplegic solution containing the cells was reduced to a volume of 1 ml. To prevent hypercontraction of the cardiomyocytes, cells were slowly acclimated to a low-calcium environment by adding volumes of a modified Tyrode solution (MT) containing (in mM): 132 NaCl, 10 HEPES/NaOH, 3.3 $MgSO_4 \times 7H_2O$, 5 KCl, 0.1 $CaCl_2$, 10 caffeine, to reach an initial concentration of 0.1% (v/v). MT volume was then incremented sequentially to 0.15%, 0.2%, 0.5% and 0.7% of the final volume. Following the last dilution, the supernatant was discarded and cells were resuspended in MT to a density of 2.5×10^4 cells/ml. Cells were gently resuspended and then allowed to sit on ice for 8 min between each dilution. Hypercontracted myocytes were readily identifiable under high-contrast brightfield illumina-

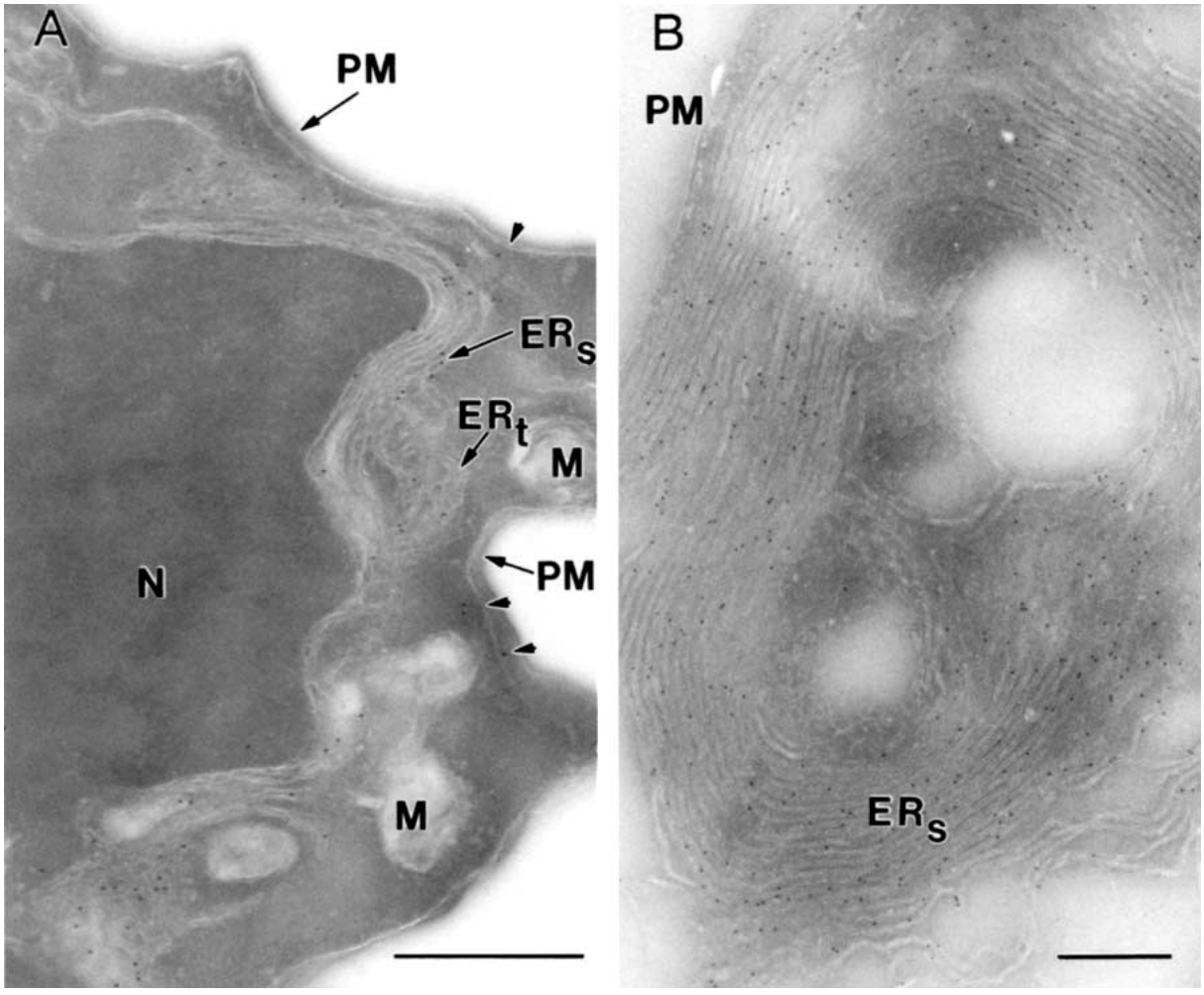

Fig. 4. Electron micrographs of HEK293 cells overexpressing hH1-GFP. Labeling of the fusion protein was performed using the anti-GFP antibody (Clontech). (*A*) Proliferation of perinuclear membrane stacks bearing hH1-GFP and tubular ER structures extending into the cytoplasm. Immunogold staining was also detected in the plasma membrane (arrowheads). (*B*) Multi-layered rings of membranes (whorls) accommodating hH1-GFP observed in the cytoplasm. Scale Bars: 0.5 μm. *PM*, plasma membrane; *M*, mitochondria; ER_S, stacked endoplasmic reticulum; ER_t, tubular endoplasmic reticulum; *N*, nucleus.

tion by their rounded ends, their general curved shape and numerous very tight and dark lines on their surface. Relaxed myocytes, on the other hand, had square edges and were fairly rectangular.

Because the plasma-membrane density of hypercontracted cells is higher along the myofilament attachment points, high amounts of sarcolemmal antigens are concentrated at the Z lines. Most antibodies then concentrate along those lines and give the impression that proteins are normally distributed along the Z lines. In control experiments, antibodies against the sodium-calcium exchanger (NCX1), KCNQ1, KCNE1, and HERG all gave identical staining along the Z lines in hypercontracted cardiomyocytes. We observed the "carpet like" distribution of NCX1 at the T tubules previously described (Chen et al., 1995) and differences in the distribution of other antigens only in relaxed myocytes. We therefore excluded hypercontracted myocytes from the analysis because of possible artefactual localization of the antigens.

One hundred ml of the final cell suspension was cytospun (Shannon Inc., PA) on precleaned glass slides (Fisher Scientific, Pittsburg, PA) and rapidly placed in a Coplin jar containing 30 ml of unbuffered alcoholic zinc fixation solution at 4°C containing: 10% ethanol, 30% acetone, 4% paraformaldehyde, (w/v) and 8 mM $ZnCl_2$, pH 3.5. Cells were fixed for 10 min at 4°C. Following several tests, we found that this composite fixative produces excellent morphological and intracellular organelle preservation as well as a "soft" protein fixation (under low calcium), conserving antigenecity.

Following fixation, cells were washed 2 × 5 min in Ca^{2+}-free Tyrode containing (in mM): 132 NaCl, 10 HEPES/NaOH, 3.3 $MgSO_4 \times 7H_2O$, 5 KCl. To facilitate access of the primary antibody to intracellular organelles, myocytes were lightly permeabilized for 5–10 min in Ca^{2+}-free Tyrode supplemented with saponin (0.25%) and CHAPS (0.5%).

Primary antibody (SP19, Sigma; directed against the conserved motif CTEEQKKYYNAMKKLGSKK) was diluted 1:200 in Ca^{2+}-free Tyrode containing 1% goat serum and applied on cells for 1.5 hr at room temperature in a humid chamber. Myocytes were then washed 3 × 5 min in Ca^{2+}-free Tyrode. Secondary antibody (goat anti-rabbit) conjugated to the green fluorescent dye Alexa 488 (Molecular Probes, OR) and propidium iodine (167 nM), a nuclear stain, were diluted 1:1000 in Ca^{2+}-free Tyrode and applied to the cells for another 1.5 hr. Cells were finally washed 2 × 5 min in

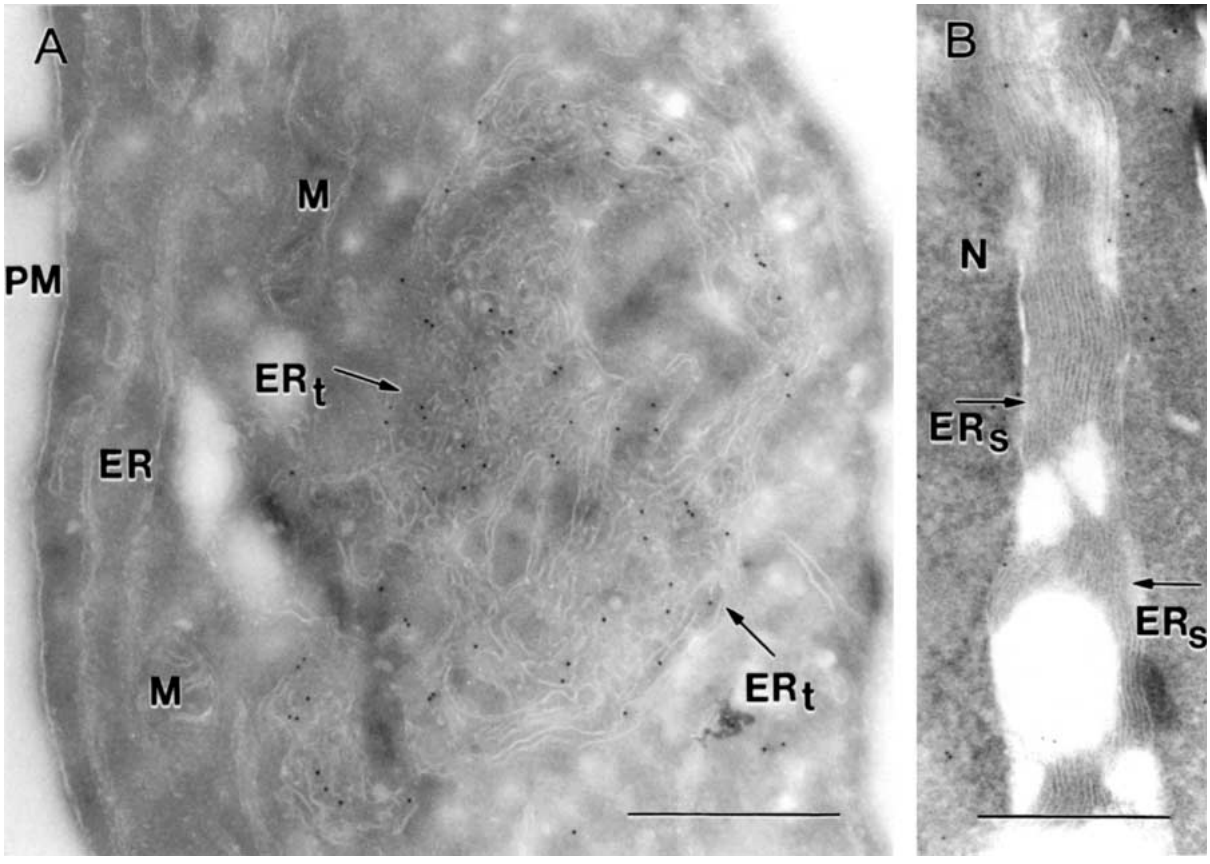

Fig. 5. Electron micrographs of HEK293 cells expressing hH1. (*A*) Transfected cell showing a tubular network of hH1-containing ER membranes (arrows). Labeling was performed using the anti-pan Na^+ channel antibody (SP19, Alomone Labs) as described in the Methods section. (*B*) Transfected cell showing growth of a perinuclear stack of ER membranes (arrows). Labeling was performed using the anti-GFP antibody (Clontech). Scale bars: 0.5 μm. *PM*, plasma membrane; *M*, mitochondria; *ER,* endoplasmic reticulum; ER_s, stacked ER; ER_t, tubular ER; *N*, nucleus.

Ca^{2+}-free Tyrode and quickly dipped (1–2 min) in acidic deionized water (pH∼5, HCl) to remove zinc salts that may have had precipitated.

Myocytes were mounted for confocal microscopy with Alexa dye Antifade Mounting Media (Molecular Probes, OR) and covered with thin coverslips.

Results

Fusion of GFP to the Human Heart Sodium Channel does not Alter Channel Function

To determine the intracellular localization of the hH1 channels in vivo, the N-terminus of GFP was fused to the COOH-terminus of hH1. The electrophysiological properties of this fusion construct (hH1-GFP) were compared with those of hH1 in transiently transfected HEK293 cells.

To insure adequate voltage control during recordings of peak currents (I_{Na}), the extracellular Na^+ concentration was reduced to 20 mM. Whole-cell currents from hH1-GFP and hH1 channels showed similar time course of activation and inactivation (Fig. 1*A*) but the amplitude of hH1-GFP peak current was, however, consistently smaller (282 ± 47 pA, n = l6, and 723 ± 86 pA, n = 29 for hH1-GFP and hH1, respectively). The voltage dependence of steady-state activation and inactivation was determined using standard electrophysiological protocols (Fig. 1*B*). The fusion of GFP had no effect on the mid-activation potential of the cardiac Na^+ channels with values of −40.1 ± 0.9 mV (n = 29) and −37.6 ± 0.6 mV (n = 16) for hH1 and hH1-GFP, respectively. The slope factor (s) was identical (6.8 ± 0.1 mV) for both constructs. We did not observe significant changes in steady-state inactivation with mean values for V_h and s of −84.3 ± 1.3 mV and 6.0 ± 0.1 mV (n = 13) for hH1, and −84.2 ± 1.2 mV and 7.0 ± 0.6 mV (n = 6) for hH1-GFP. Thus, linking GFP to the C-terminus of hH1 did not alter the voltage dependence of activation or the availability of the channels.

We next investigated whether GFP affected the kinetics of inactivation. To this end, we fitted the decay of I_{Na} to a monoexponential or a biexponential

function. When fitted to a sum of two exponentials, the slow component in the current decay accounted for less than 15% of the peak amplitude and appeared in both hH1 and hH1-GFP current recordings. For statistical analysis, the dominating fast time constant of the biexponential fits and the time constants of the monoexponential fits were lumped together and the mean τ_h was plotted as function of voltage (Fig. 1*C*). Our results show that the time course of inactivation (current decay) was not altered by GFP.

We compared the single-channel activity of both channels in cell-attached patches depolarized to −40 mV from a holding potential of −120 mV. Fig. 2 shows representative current recordings from hH1 and hH1-GFP channels. Amplitude histograms fitted with Gaussian functions (*not shown*) revealed average single-channel amplitudes of 2.0 ± 0.1 pA ($n = 4$) and 1.9 ± 0.1 pA ($n = 3$) for hH1 and hH1-GFP channels, respectively. We also regularly observed smaller-amplitude openings in both channels (*see* fifth trace in hH1 and fourth trace in hH1-GFP). The most frequent sublevel amplitude was 0.9 pA. We concluded that GFP did not affect the single-channel conductance of hH1.

hH1-GFP and hH1 are Abundant in Intracellular Membranes and Induce Proliferation of the ER

We studied the intracellular distribution of hH1-GFP in HEK293 cells by means of confocal laser-scanning microscopy. The cells were transfected by lipofection and the appearance of the GFP-fluorescence signal was monitored in situ. In all transfected cells a significant accumulation of dense green spots was already observed 1 to 2 hours after transfection. After fifteen hours, the fluorescent signal was predominantly located in three types of intracellular structures and remained strong for up to 48 hours (Fig. 3). All transfected cells showed the following: (1) a fine fluorescent network throughout the cytoplasm, (2) intensely labeled semicircle-like plates (arrows in Fig. 3*A*) and/or (3) spherical structures (Fig. 3*A*, far right). Independent staining of the plasma membrane with the dye FM1-43 showed that these intracellular structures could be clearly distinguished from the plasma membrane but were sometimes localized in its close vicinity (Fig. 3*B*). Compared to the intracellular structures, the plasma membrane showed fainter green fluorescence (Fig. 3*B*), indicating a smaller portion of electrophysiologically active hH1-GFP channels at the surface of the cell. To more specifically link the intracellular expression of hH1-GFP and hH1 to intracellular organelles and to characterize hH1-induced changes in subcellular membranes, we investigated transiently transfected cells by immuno-electronmicroscopy.

Fig. 4 shows that expression of hH1-GFP induced proliferation of three types of ER membrane structures: A tubular network (Fig. 4*A*), densely packed stacks of membranes frequently located close to the nucleus (Fig. 4*A*), and cytoplasmic multi-layered membrane whorls (Fig. 4*B*). Immunogold-labeling using the anti-GFP antibody showed that all these structures accommodated the hH1-GFP fusion protein. Specific immunogold labeling also indicated that hH1-GFP is present, although at a lower density, in the plasma membrane (arrowheads in Fig. 4*A*). Expression of wild-type hH1 similarly induced proliferation of three morphologically distinct ER subcompartments (Fig. 5), not observed in untransfected cells. However, we found more hH1-transfected cells containing an extensive tubular network (Fig. 5*A*), and membrane stacks (Fig. 5*B*) were less frequently observed. Immunogold-labeling of hH1 (Anti-Pan α from Alomone Labs) revealed a distribution pattern similar to hH1-GFP, with the protein preferentially located in the same proliferated membrane structures (Fig. 5*A*). Specific labeling of hH1 was also observed in the plasma membrane (*not shown*) but, as with hH1-GFP, was not as dense as in intracellular membranes. The ratio between immunogold labeling of intracellular membranes to plasma membrane was 1601 to 25 and 342 to 9, when assessed by counting all immunogold grains in 24 hH1-GFP- and 9 hH1-transfected cells, respectively. This indicates that the amount of sarcolemmal protein accounted for only 2% and 3% of the total amount of hH1-GFP and hH1, respectively, present in the cell and suggests an intracellular storage mechanism.

Thus, the proliferation of three different ER compartments and the preferential localization of hH1 within these membranes are not linked to GFP, but to the expression of hH1.

The Native Na^+-Channel Protein Accumulates in Perinuclear Membranes of Dog Cardiomyocytes

The localization of hH1 and hH1-GFP in intracellular membranes of transfected HEK293 cells raised the question whether or not a similar distribution of native Na^+ channels exists in cardiac ventricular cells. Immunofluorescence experiments using the SP19 polyclonal antibody directed against a conserved region within the cytosolic III–IV loop of voltage-gated Na^+ channels revealed a strong labeling of the surface of dog cardiomyocytes along Z lines and also around T tubules, as previously described (Fig. 6*A*; Cohen, 1996). Strong labeling was also observed in putative areas of intercellular contact forming the intercalated disks (arrowheads in Fig. 6*A*).

We observed a strong staining of intracellular membrane structures (Fig. 6*A–C*) not previously de-

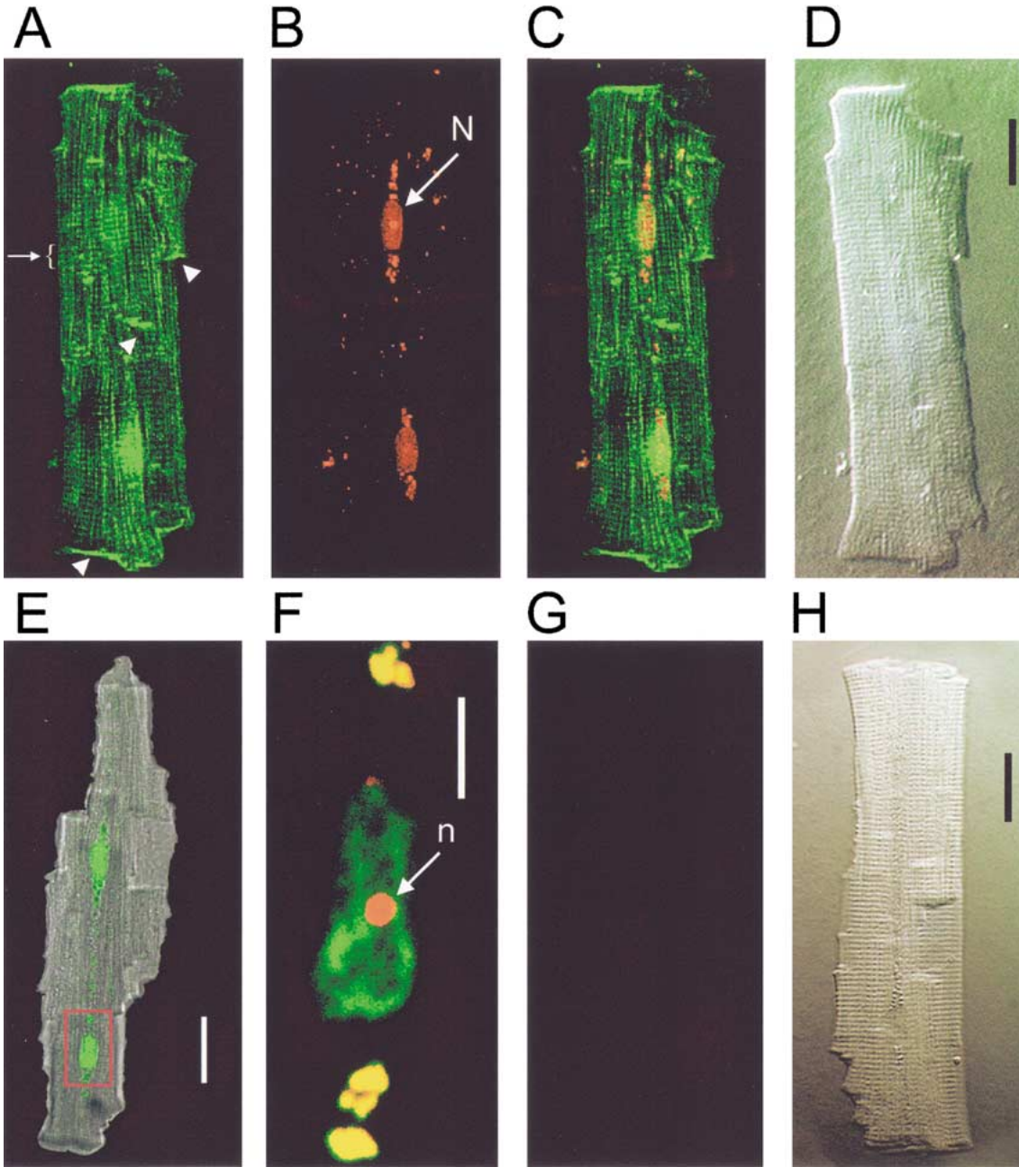

Fig. 6. An intracellular Na^+-channel α-subunit pool exists in native cardiomyocytes. Dog cardiac myocytes from the left ventricle were probed with a polyclonal Na^+ channel antibody (SP19 from Sigma) detected with a secondary antibody conjugated to Alexa 488 dye (FITC) and counterstained with propidium iodine (PI). (*A*) Series of 26 optical sections between 0.6 and 0.8 μm thickness were taken from a representative myocyte in fluorescence mode and superimposed. Vertical step increments: 0.3 μm. The green signal corresponds to detection of the SP19 antibody by the Alexa 488-conjugated goat anti-rabbit secondary antibody (Molecular Probes). Arrowheads indicate areas forming the intercalated disks. Arrow indicates linear staining along the Z lines. (*B*) Florescence from propidium iodine indicates areas rich in RNA and DNA. Propidium iodine strongly stained the nucleus (*N*) and localized intracellular regions in red. (*C*) Series of 26 optical sections as described in *A*, taken with the confocal microscope configured to simultaneously record fluorescence from the (SP19) antibody and the nuclear dye. Na^+ channel proteins (green) are more abundant in the nuclear region where intense yellow staining (red + green) is observed. (*D*) Bright-field image in transmitted light (Nomarski interference contrast) of the myocyte described in *A–C*. *(E)* Confocal image series as in *A* and *B* recorded simultaneously in transmitted and fluorescence mode. (*F*) The region enclosed by the red square in panel *E* is shown here at higher magnification. The image is from a 1-μm thick optical section taken 8 μm from the sarcolemmal surface and showing a high concentration of Na^+-channel proteins (green) detected in a region surrounding the chromatin-rich nucleolus of the cell (*n*) at the center of the nuclear sac (*N*), as presented in panel *B*. In that particular set of experiments, all solutions were supplemented with RNAse to more specifically stain the chromosomal DNA present in the nucleolus. (*G*) Control staining with SP19 immune sera (1:200 dilution) pre-absorbed against the sodium channel antigen. (*H*) Myocyte presented in *G* viewed in bright-field transmitted light (Nomarski interference contrast). Scale bars *A–E*, *H*: 20 μm, *F*: 5 μm.

scribed in native cardiomyocytes, but similar to what was observed in HEK293 cells transfected with hH1 or hH1-GFP. These structures appeared in an area corresponding to the membrane of the nuclear sac (*N*) commonly referred to as the nucleus (Fig. 6*A–D*) and in close periphery to the cell nucleolus (*n*), as confirmed by simultaneous staining of chromosomal DNA with propidium iodine (Fig. 6*F*). Analogous to the distribution of hH1 observed in transfected HEK293 cells, native Na^+ channels were less abundant, but still present, in the sarcolemmal membrane of cardiomyocytes. In Fig. 6*F*, sarcolemmal channels are out of sight because of the depth (~8 μm) at which the optical section was taken, the confocal aperture, and the lower photomultiplier sensitivity used to avoid saturation. Yellow areas (red + green) indicate regions where DNA or RNA and the channel protein were in close proximity. These data indicate that a significant fraction of the Na^+ channel protein is stored in intracellular membrane structures of cardiac myocytes close to the nuclei, a phenomenon similar to what we observed in HEK293 cells (Figs. 3–5).

hH1 Preferentially Accumulates in the ER and not in the Golgi Apparatus

The accumulation of hH1-GFP within intracellular membranes and its low incidence in the plasma membrane suggest the presence of a rate-limiting step in the trafficking of the protein from the ER to the plasma membrane. To address this question, we coexpressed hH1-GFP with a specific marker of either the ER (CFP-ER) or the Golgi apparatus (YFP-Golgi). Fig. 7 shows confocal images of fluorescent structures differentially recognized by expressing either CFP-ER (*A*) or YFP-Golgi (*B*) in control cells. To simultaneously detect each of these markers and hH1 we exchanged GFP in hH1-GFP for either YFP or CFP and coexpressed the construct with the specific organelle marker of interest. When we coexpressed hH1-YFP and CFP-ER, we found that the two gene products highlighted similar intracellular structures (Fig. 7*C*). An intensity profile along one axis of a representative HEK293 cell (Fig. 7*D*) showed the close spatial correlation existing between the intensity distribution of hH1-YFP and CFP-ER fluorescence, thus confirming the localization of both proteins within the ER. When comparing both hH1-YFP fluorescence peaks in the profile pattern with those of CFP-ER (Fig. 7*D*) we noticed stronger fluorescence signals at 3 μm for hH1-YFP and at 14 μm for CFP-ER. This shows that the concentration of hH1-YFP and/or CFP-ER was different in different ER compartments.

When we repeated the coexpression experiments using the combination hH1-CFP and YFP-Golgi, the yellow fluorescence indicating the localization of the Golgi apparatus did not correlate with the strong cyan fluorescence of hH1-CFP (Fig. 7*E*). The channel was again mainly localized within plates of membranes and within the tubular membrane network — membrane structures that belong to the ER (*compare* Figs. 4 and 5 with Fig. 7*C*). An intensity profile (Fig. 7*E*) revealed a multiple-peak fluorescence pattern for hH1-CFP that did not coincide with the signal obtained for YFP-Golgi. Only a small portion of the channel was found within Golgi membranes (Fig. 7*F*). Occasionally, a low fluorescence signal from the Golgi marker was also present in the hH1-CFP-containing ER structures (*not shown*) because the YFP-Golgi protein had to be synthesized within the ER before being transported to the trans-medial region of the Golgi apparatus (*see* Golgi structures in Fig. 7*B*).

Thus, intracellular hH1 channels were predominantly localized within the ER, whereas in the Golgi apparatus the density of channel molecules was very low. This suggests the presence of rate-limiting steps in the trafficking of the channel possibly taking place before the proteins reach the trans-medial Golgi region.

Discussion

In the present study, we describe an experimental model for studying the subcellular localization of the human heart Na^+ channel heterologously expressed in a mammalian cell line. We found that hH1 induced proliferation of distinct ER subcompartments and evidence suggesting that the pathway from the ER to the Golgi apparatus involves rate-limiting steps in hH1 trafficking to the plasma membrane.

We also show that the hH1-GFP fusion protein represents a useful model to investigate relevant aspects of the hH1 biogenesis as its electrophysiological properties and subcellular localization were comparable to those of hH1. From our electrophysiological measurements we conclude that hH1-GFP channels are targeted appropriately to the plasma membrane. Furthermore, immuno-electronmicroscopy showed that most of the hHl protein is located in three morphologically distinct ER structures that were independently induced, whether by hHl or hHl-GFP expression. Our data also show that a small fraction of all the channels synthesized is targeted to the plasma membrane and needed to produce strong inward current. However, this portion seems to be lower in hHl-GFP. This conclusion was derived from the lower incidence of hHl-GFP channels in the electron micrographs and it fits also with the smaller whole-cell currents (Fig. 1) at an unchanged single-channel conductance (Fig. 2). Possible explanations are (1) that the open probability is lower in hHl-GFP or (2) that hHl-GFP is subject to a higher turnover, due to a partially disturbed tertiary structure.

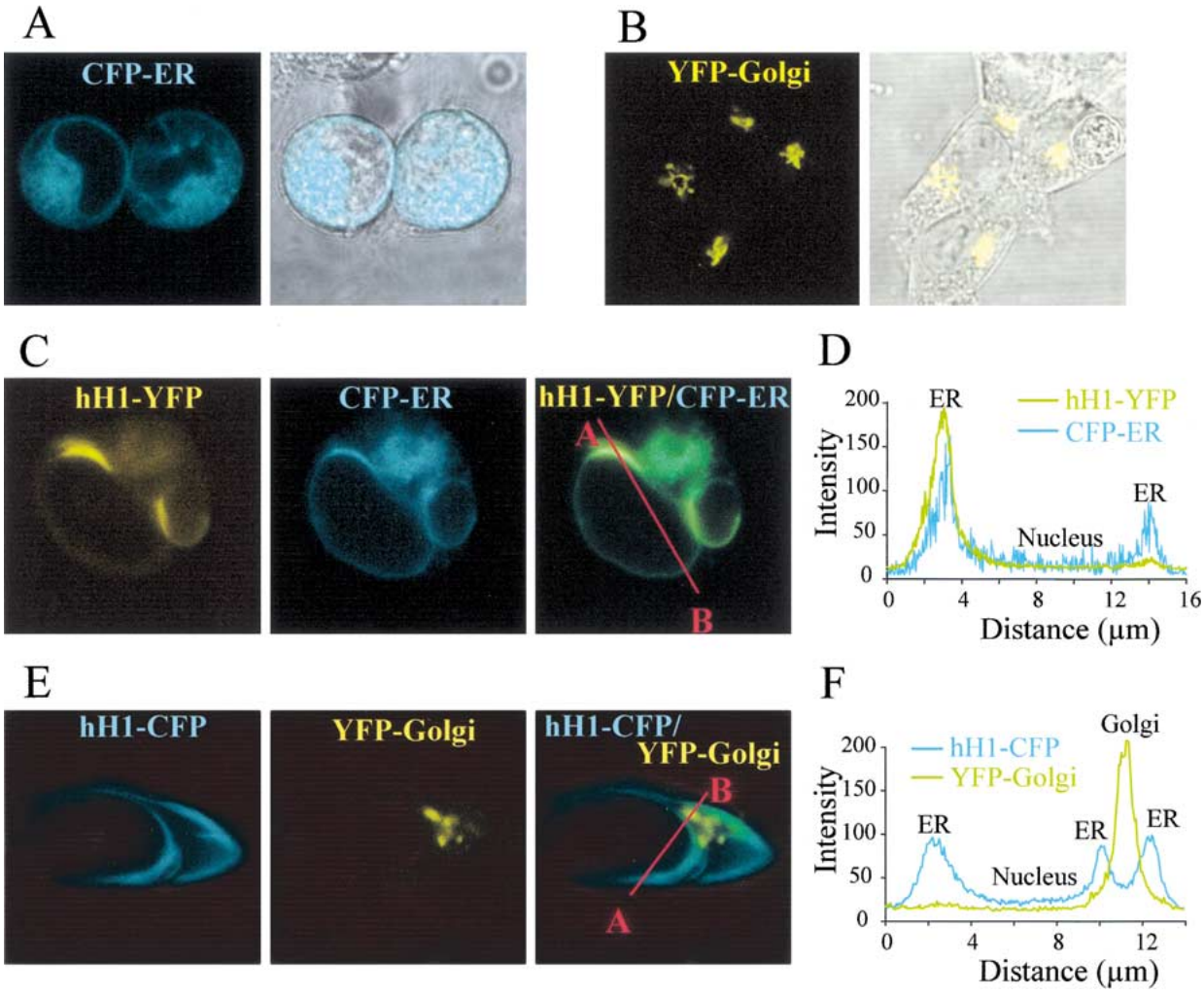

Fig 7. Predominant localization of hHl in the ER, but not in the Golgi apparatus. Specific fluorescence labeling of the endoplasmic reticulum (*A*) and the Golgi apparatus (*B*) in HEK293 cells expressing CFP-ER and YFP-Golgi, respectively (*see* Methods). Cells were transfected either by pECFP-ER (*A*) or pEYFP-Golgi (*B*) to localize the respective organelles in control cells. The fluorescence patterns (*A* and *B*, left panels) were superimposed on the corresponding transmitted image (*A* and *B*, right panels). (*C*) Labeling of the ER with CFP-ER in a cell expressing hH1-YFP. (*D*) Distribution of hH1-YFP and CFP-ER in the double-labeled ER membrane compartments. The intensity profiles were obtained by plotting the fluorescence intensity, in arbitrary units, against the distance of the pixel from A on the cell axis to B (red line in *C*). (*E*) Labeling of the Golgi apparatus with YFP-Golgi in a representative cell expressing hH1-CFP. (*F*) The intensity profiles demonstrate the fluorescence distribution of hH1-CFP and YFP-Golgi for the cell shown in *E* (red line from A to B).

Questions as to the physiological significance of the hHl-induced proliferation of the ER naturally arise. ER proliferation has been mainly investigated in the context of ER biogenesis (reviewed in Sandig et al., 1999; Takewaka et al., 1999) and, to our knowledge, has never been reported in response to expression of a voltage-gated ion channel. Previous studies suggest that ER proliferation occurs naturally when growth conditions, environmental stress or other factors require the enhanced production of a distinct metabolically active protein. Examples for such a physiological enlargement of the ER are the phenobarbital-induced overexpression of hepatic cytochromes P450 resulting in proliferation of tubular ER (Orrenius, Erricson & Ernster, 1965; Frueh, Zanger & Meyer, 1997), enhanced production of the inositol 1,4,5-trisphosphate receptor in Purkinje neurons of the cerebellum, resulting in the proliferation of stacks of ER cisternae (Takei et al., 1992), and induction of alkane hydroxylases by alkanes or fatty acids in *Candida* species, resulting in a general expansion of the ER (Vogel et al., 1992).

Similar ER structures also evolved when such a membrane protein was expressed in a heterologous host (reviewed in Sandig et al., 1999). Moreover, it is currently believed that such heterologous expression induces growth of pre-existing ER membrane compartments involved in trafficking, storage, or degradation of membrane proteins. Our immunoelectronmicroscopy data clearly show that hHl has

the ability to induce proliferation of morphologically distinct ER structures. We frequently observed stacks of ER membranes in close vicinity to the nucleus when investigating hHl-GFP- or hHl-expressing cells. The fluorescent structures described in this study appeared in all transfected cells also when significantly less plasmid DNA was used for the transfection procedure (0.2 μg per transfection), suggesting that the associated ER proliferation is not simply an artefact from overexpression and ER saturation with hHl-GFP.

In cardiomyocytes, the sodium channels were found to be preferentially distributed at the T tubules as well as along the Z lines. Strong staining was also observed in cell-to-cell contact areas along the longitudinal axis and at both ends of the myocytes, in regions likely to form intercalated disks, as previously reported (Cohen, 1996; Malhotra et al., 2001). In addition, we observed a strong staining of intracellular organelles by the SP19 antibody not previously described and akin to the perinuclear distribution observed in neurons. Although the SCN5A isoform is the predominantly expressed Na^+ channel in the heart, the SP19 antibody used in this study may also recognize other Na^+ channel isoforms that may be present in cardiomyocytes (Malhotra et al., 2001; Zimmer et al., 2001). This issue was not experimentally addressed in the present paper, but as subtype-specific antibodies become commercially available, colocalization of the different isoforms in native cardiomyocytes should solve this issue. Nonetheless, the heterologous expression experiments showing that hHl (SCN5A) accumulates also in intracellular organelles strongly suggest that this process is an intrinsic property of voltage-dependent Na^+ channels. This idea is substantiated by previous reports that demonstrated the presence of a large intracellular pool of Na^+ channel α subunits in developing neurons of rat brain (Schmidt & Catterall, 1986) and a cytoplasmic labeling of Na^+ channels in rat myocytes (Cohen, 1996). We therefore favor the idea that much of the intracellular signal from the SP19 antibody corresponds to recognition of the SCN5A channel antigen.

Our results indicate that the ER serves as a Na^+-channel reservoir that under physiological conditions may be involved in the rapid increase of sarcolemmal Na^+-channel density during stimulation by PKA (Lu et al., 1999; Zhou et al., 2000) and could play a role in the adrenergic modulation of cardiac conduction (Zuanetti, Hoyt & Corr, 1990; Munger, Johnson & Packer, 1994). Further experiments are needed to confirm this hypothesis.

In the Golgi apparatus of transfected cells, in which voltage-gated Na^+ channels become highly glycosylated (Schmidt & Catterall, 1986 and 1987), we detected a low fluorescence signal from the optically labeled hHl. This indicates that the processing of newly synthesized α subunits in the ER or trafficking between the ER and the trans-medial region of the Golgi apparatus are rate-limiting factors in the cell-surface expression of Na^+ channels. Similar to inwardly rectifying potassium channels (Zerangue et al., 2000; Ma et al., 2001), compartimentalization within the ER or forward trafficking of the protein is likely to involve specific hHl sequence motifs. In this respect it is interesting to note the recent work by Zhou et al. (2000) who suggest that the interdomain I–II linker may be involved in the PKA-induced increased expression of hHl in the plasma membrane of *Xenopus* oocytes. Heterologous expression of hHl-GFP in HEK293 cells could therefore provide mechanistic insight into retention/trafficking motifs in hHl involved in the ER retention and the expression of native Na^+ channels.

Finally, we conclude, that heterologous expression of hHl-GFP in HEK293 cells presents several of the biosynthesis features previously found in native cardiac or neuronal cells and represents a valuable model to investigate translational mechanisms involved in the expression of cardiac sodium channels.

The authors thank Dr. George and Dr. Kallen for the hHl cDNA. We are also very grateful to K. Schoknecht, A. Kolchmeier, H. Rietzke, J. Hefferon and Dr. Arthur Iodice for excellent technical assistance. This work was supported by a grant form the Deutsche Forschungsgemeinschaft (Be1250/9-2) and by NIH grant # HL59449 to R.D.

References

Benndorf, K. 1995. Low noise recording. *In* Single-Channel Recording. B. Sakmann, E. Neher, editors. pp. 129–145. Plenum Press New York

Böhle, T., Benndorf, K. 1994. Facilitated giga-seal formation with a just originated glass surface. *Pfluegers Arch.* **427:**487–491

Böhle, T., Steinbis, M, Biskup, C, Koopmann, R., Benndorf, K. 1998. Inactivation of single cardiac Na^+ channels in three different gating modes. *Biophys. J.* **75:**1740–1748

Brammar, W.J. 1999. Voltage-gated sodium channels. *In*: The ion channel facts book IV. Conley, B.C., Brammar W.J., editors, pp. 768–838. Academic Press, London

Catterall, W.A. 1992. Cellular and molecular biology of voltage-gated sodium channels. *Physiol. Rev.* **72:**S15–S48

Chen, F., Mottino, G., Klitzner, T.S., Philipson, K.D., Frank, J.S. 1995. Distribution of the Na^+/Ca^+ exchange protein in developing rabbit myocytes. *Am. J. Physiol.* **268:**C1126–C1132

Cohen, S.A. 1996. Immunocytochemical localization of rHl sodium channel in adult rat heart atria and ventricle. Presence in terminal intercalated disks. *Circulation* **94:**3083–3086

Frueh, F.W., Zanger, U.M., Meyer, U.A. 1997. Extent and character of phenobarbital-mediated changes in gene expression in the liver. *Mol. Pharmacol.* **51:**363–369

Gellens, M.E., George Jr., A.L., Chen, L., Chahine, M., Horn, R., Barchi, R.L., Kallen, R.G. 1992. Primary structure and functional expression of the human cardiac tetrodotoxin-insensitive voltage-dependent sodium channel. *Proc. Natl. Acad. Sci. USA* **89:**554–558

Hamill, O.P., Marty, A., Neher, E., Sakmann, B., Sigworth, F.J. 1981. Improved patch-clamp techniques for high-resolution

current recording from cells and cell-free membrane patches. *Pfluegers Arch.* **391:**85–100

Heathers, G.P., Yamada, K.A., Kanter, E.M., Corr, P.B. 1987. Long-chain acylcarnitines mediate the hypoxia-induced increase in alpha-1 adrenergic receptors on adult canine myocytes. *Circ. Res.* **61:**735–746

Kazen-Gillespie, K.A., Ragsdale, D.S., D'Andrea, M.R., Mattei, L.N., Rogers, K.E., Isom, L.L. 2000. Cloning , localization, and functional expression of sodium channel β_{1A} subunits. *Biol. Chem.* **275:**1079–1088

Lu, T., Lee, H.C., Kabat, J.A., Shibata, E.F. 1999. Modulation of rat cardiac sodium channel by the stimulatory G protein alpha subunit. *J. Physiol.* **518:**371–384

Ma, D., Zerangue, N., Lin, Y.-F., Collins, A., Yu, M., Jan, Y.N., Jan, L.Y. 2001. Role of ER export signals in controlling surface potassium channel numbers. *Science* **291:**316–319

Malhotra, J.D., Chen, C,, Rivolta, I, Abriel, H., Malhotra, R., Mattei, L.N., Brosius, F.C., Kass, R.S., Isom, L.L. 2001. Characterization of sodium channel α- and β-subunits in rat and mouse cardiac myocytes. *Circulation* **103:**1303–1310

Morgan, K., Stevens, E.B., Shah, B., Cox, P.J., Dixon, A.K., Lee, K., Pinnock, R.D., Hughes, J., Richardson, P.J., Mizuguchi, K., Jackson, A.P. 2000. β_3: An additional auxiliary subunit of the voltage-sensitive sodium channel that modulates channel gating with distinct kinetics. *Proc. Natl. Acad. Sci. USA* **97:**2308–2313

Munger, T.M., Johnson, S.B., Packer, D.L. 1994. Voltage dependence of beta-adrenergic modulation of conduction in the canine Purkinje fiber. *Circ. Res.* **75:**511–519

Orrenius, S., Ericsson, J.L.E., Ernster, L. 1965. Phenobarbital-induced synthesis of the microsomal drug-metabolizing enzyme system and its relationship to the proliferation of endoplasmic membranes. A morphological and biochemical study. *J. Cell. Biol.* **25:**627–639

Sambrook, J., Fritsch, E.F., Maniatis, T. 1989. Molecular Cloning: A Laboratory Manual. Cold Spring Harbor Laboratory Press, Cold Spring Harbor NY

Sandig, G., Kärgel, E., Menzel, R., Vogel, F., Zimmer, T., Schunck, W.H. 1999. Regulation of endoplasmic reticulum biogenesis in response to cytochrome P450 overproduction. *Drug. Met. Rev.* **31:**393–410

Sanger, F., Nicklen, S., Coulsen, A.R. 1977. DNA sequencing with chain-terminating inhibitors. *Proc. Natl. Acad. Sci. USA.* **74:**5463–5467

Schmidt, J.W., Catterall, W.A. 1986. Biosynthesis and processing of the alpha subunit of the voltage-sensitive sodium channel in rat brain neurons. *Cell* **46:**437–445

Schmidt, J.W., Catterall, W.A. 1987. Palmitylation, sulfation, and glycosylation of the alpha subunit of the sodium channel. Role of post-translational modifications in channel assembly. *J. Biol. Chem.* **262:**13713–13723

Takei, K., Stukenbrok, H., Metcalf, A., Mignery, G.A., Südhof, T.C., Volpe, P., De Camilli, P. 1992. Ca^{2+} stores in Purkinje neurons: endoplasmic reticulum subcompartments demonstrated by the heterogeneous distribution of the InsP3 receptor, Ca^{2+}-ATPase, and calsequestrin. *J. Neurosci.* **12:** 489–505

Takewaka, T., Zimmer, T., Hirata, A., Ohta, A., Takagi, M. 1999. Null mutation in *IRE1* gene inhibits overproduction of microsomal cytochrome P450Alkl (CYP 52A3) and proliferation of the endoplasmic reticulum in *Saccharomyces cerevisiae*. *J. Biochem.* **125:**507–514

Tokuyasu, K.T. 1989. Use of poly(vinylpyrrolidone) and poly (vinyl alcohol) for cryoultramicrotomy, *Histochem. J.* **21:**163–171

Vogel, F., Gengnagel, C., Kärgel, E., Müller, H.-G., Schunck, W.-H. 1992. Immunocytochemical localization of alkane-inducible cytochrome P-450 and its NADPH-dependent reductase in the yeast *Candida maltosa*. *Eur. J. Cell Biol.* **57:**285–291

Zerangue, N., Schwappach, B., Jan, Y.N., Jan, L.Y. 2000. A new trafficking signal regulates the subunit stoichiometry of plasma membrane K_{ATP} channels. *Neuron* **22:**537–548

Zhou, L, Yi, J., Hu, N., George Jr., A.L., Murray, K.T. 2000. Activation of protein kinase A modulates trafficking of the human cardiac sodium channel in *Xenopus* oocytes. *Circ. Res.* **87:**33–38

Zimmer, T., Birch-Hirschfeld, E., Bollensdorff, C., Benndorf, K. 2001. Sodium channels in the mouse heart: Cloning and characterization of two distinct isoforms and alternatively spliced variants. *Biophys. J.* **80:**892

Zuanetti, G., Hoyt, R.H., Corr, P.B. 1990. Beta-adrenergic-mediated influences on microscopic conduction in epicardial regions overlying infarcted myocardium. Circ. *Res.* **67:**284–302

Zygmunt, A.C., Goodrow, R.J., Weigel, C.M. 1998. I_{NaCa} and $I_{Cl(ca)}$ contribute to isoproterenol-induced delayed afterdepolarizations in midmyocardial cells. *Am. J. Physiol.* **275:**H1979–H1992